A Timeline of Bacterial and Archaeal Diversification in the Ocean

Carolina A. Martinez-Gutierrez[1*], Josef C. Uyeda[1], Frank O. Aylward[1,2*]
1 Department of Biological Sciences, Virginia Tech, Blacksburg, VA, USA
2 Center for Emerging, Zoonotic, and Arthropod-borne Pathogens, Virginia Tech, Blacksburg, VA, USA

*Email for correspondence:
Frank O. Aylward: faylward@vt.edu; Carolina A. Martinez-Gutierrez: cmartinez@vt.edu

ABSTRACT

Microbial plankton play a central role in marine biogeochemical cycles, but the timing in which abundant lineages colonized contemporary ocean environments remains unclear. Here, we reconstructed the geological dates in which major clades of bacteria and archaea colonized the ocean using a high-resolution benchmarked phylogenetic tree that allows for simultaneous and direct comparison of the ages of multiple divergent lineages. Our findings show that the diversification of the most prevalent marine clades is the result of three main phases of colonization that coincide with major oxygenation events. The first phase took place after the initial oxygenation of the planet that occurred at the time of the Great Oxidation Event (2.4-2.2 Ga), after which several lineages that proliferate in oxygen minimum zones today first colonized marine niches. The second phase began around the time of the Neoproterozoic Oxidation Event (0.8-0.4 Ga) and included the diversification of the most abundant heterotrophic bacterial clades, consistent with the hypothesis that their diversification is linked to the emergence of large eukaryotic phytoplankton. The last phase encompasses prevalent cyanobacterial lineages and occurred after the Phanerozoic Oxidation Event (0.45-0.4 Ga), coinciding with the formation of the contemporary oligotrophic ocean. Our work clarifies the timing at which abundant lineages of bacteria and archaea colonized the ocean, links their adaptive radiations with key geological events, and

demonstrates that the redox state of the ocean throughout Earth's history has been the primary factor shaping the diversification of the most prevalent marine microbial clades.

Keywords: Microbial Oceanography, Marine Microbial Diversification, Bayesian Molecular Dating, Great Oxidation Event

MAIN TEXT

The ocean plays a central role in the functioning and stability of Earth's biogeochemistry[1–3]. Due to their abundance, diversity, and physiological versatility, microbes mediate the vast majority of organic matter transformations that underpin higher trophic levels[1,2,4,5]. For example, marine microorganisms regulate a large fraction of the organic carbon pool[6], drive elemental cycling of nutrients like nitrogen[7], and participate in the ocean-atmosphere exchange of climatically important gasses[8]. Starting in the 1980s, analysis of small-subunit ribosomal RNA genes began to reveal the identity of dominant clades of bacteria and archaea that were notable for their ubiquity and high abundance, and subsequent analyses highlighted their diverse physiological activities in the ocean[9]. Phylogenetic studies showed that these clades are broadly distributed across the Tree of Life (ToL) and encompass a wide range of phylogenetic breadths[9]. Cultivation-based studies and the large-scale generation of genomes from metagenomes have continued to make major progress in examining the genomic diversity and metabolism of these major marine clades, but we still lack a comprehensive understanding of the evolutionary events leading to their origin and diversification in the ocean.

51 Several independent studies have used molecular phylogenetic methods to date the diversification
52 of some marine microbial lineages, such as the Ammonia Oxidizing Archaea of the order
53 *Nitrososphaerales* (Marine Group I, MGI)[10,11], picocyanobacteria of the genera *Synechococcus*
54 and *Prochlorococcus*[12–14], and marine alphaproteobacterial groups that included the SAR11 and
55 Roseobacter clades[15]. Differences in the methodological frameworks used in these studies often
56 hinder comparisons between lineages, however, and results for individual clades often conflict[10–
57 13]. Moreover, it has been difficult to directly compare bacterial and archaeal clades due to the vast
58 evolutionary distances between these domains. For these reasons it has remained challenging to
59 evaluate the ages of different marine lineages and develop a comprehensive understanding of the
60 timing of microbial diversification events in the ocean and their relationship with major geological
61 events throughout Earth's history.
62
63 To address these challenges, we constructed a multi-domain phylogenetic tree that allowed us to
64 directly compare the origin of 13 planktonic marine bacterial and archaeal clades that are known
65 for their abundance and major roles in marine biogeochemical cycles in the modern ocean (Fig.
66 1). We based tree reconstruction on a benchmarked set of marker genes that we have previously
67 shown to be congruent for inter-domain phylogenetic reconstruction[16] (details in Methods,
68 Supplemental File 2). Our phylogenetic framework included non-marine clades for phylogenetic
69 context, and overall it recapitulates known relationships across the ToL, such as the clear
70 demarcation of the Gracilicutes and Terrabacteria superphyla in Bacteria and the basal placement
71 of the *Thermatogales*[16,17] (Fig. 1). To gain insight into the geological landscape in which these
72 major marine clades first diversified, we performed a Bayesian relaxed molecular dating analysis
73 on our benchmarked ToL using several calibrated nodes (Fig. 1 and Table 1). Due to the limited

representation of microorganisms in the fossil record and the difficulties to associate fossils to taxonomic groups, we employed geochemical evidence as temporal calibrations (Fig. 1 and Table 1). Moreover, because of the uncertainty in the length of the branch linking bacteria and archaea, the crown node for each domain was calibrated independently. We used the age of the presence of liquid water as approximated through the dating of zircons[18], as well as the most ancient record of biogenic methane[18,19] as maximum and minimum prior ages for bacteria and archaea (4400 and 3460 My, respectively, Fig. 1 and Table 1). For internal calibration, we used the recent identification of non-oxygenic Cyanobacteria to constrain the diversification node of oxygenic Cyanobacteria with a minimum age of 2320 My, the estimated age for the Great Oxidation Event (GOE)[20–22]. Similarly, we applied this reasoning for the calibration of the crown group of aerobic Ammonia Oxidizing Archaea, aerobic *Ca.* Marinimicrobia, and the Nitrite Oxidizing Bacteria, using their strict aerobic metabolism as evidence for a maximum of 2320 My. Our Bayesian estimates are consistent with the ancient origin of major bacterial and archaeal supergroups, such as Asgardarchaeota, Euryarchaeota, Firmicutes, Actinobacteria, and Aquificota (Fig. 2). Moreover, the date we found for oxygenic Cyanobacteria (2597 My; Fig. 2) is in agreement with geological evidence that points to their diversification happening before the GOE[23].

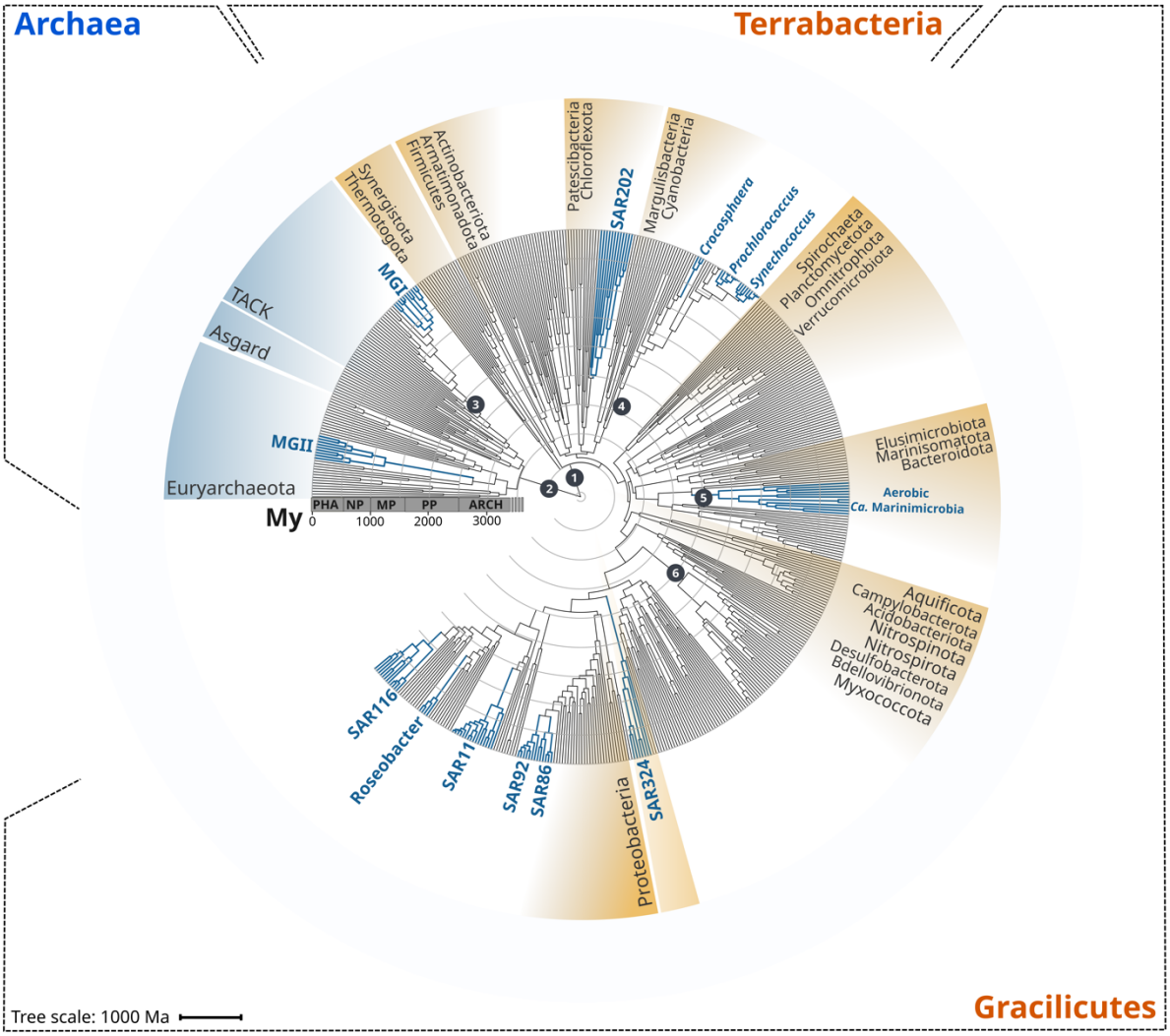

Figure 1. Rooted inter-domain Tree of Life used for molecular dating analyses. Maximum likelihood tree constructed in IQ-TREE v1.6.12 using the concatenation of 30 RNAP subunits and ribosomal protein sequences and the substitution model LG+R10. Blue labels represent the marine clades dated in our study. Dark gray dots show the temporal calibration used in our molecular dating analyses (Table 1). The marine clades shown are classified on the GTDB as follows: MGII, *Poseidoniales;* MGI, *Nitrososphaerales*; SAR202, SAR202; *Crocosphaera, Crocosphaera*; *Prochlorococcus, Prochlorococcus*; *Synechococcus, Synechococcus*; *Ca.* Marinimicrobia, *Marinisomatia*; SAR324, SAR324; SAR86, *Oceanospirillales*; SAR92, *Porticoccaceae*; SAR11, *Pelagibacterales*; Roseobacter, *Rhodobacteraceae*; SAR116, *Puniceispirillaceae.*

Table 1. Temporal calibrations used as priors for the molecular dating of the main marine microbial clades.

Node	Calibration group	Minimum (MY)	Maximum (MY)	Evidence	Reference
1,2	Bacteria-Archaea Root	-	4400	Identification of the most ancient zircons showing evidence of liquid water.	*17*
1,2	Bacteria-Archaea Root	3460	-	Identification of the most ancient traces of methane.	*18*
3	Aerobic *Nitrososphaerales*	-	2320	Strict aerobic metabolism.	*19*
4	Oxygenic Cyanobacteria	2320	-	Oxygenation of the atmosphere. The Great Oxidation Event has been associated with oxygenic Cyanobacteria.	*19*
5	Aerobic *Ca.* Marinimicrobia	-	2320	Strict aerobic metabolism.	*19*
6	Nitrite oxidizing bacteria	-	2320	Strict aerobic metabolism.	*19*

The ages of marine bacterial and archaeal clades demonstrates that their diversification can be broadly divided into three phases that coincide with the major oxygenation events of the atmosphere and the ocean (Fig. 2). The first phase occurred near the time of the GOE, and included the clades SAR202, aerobic *Ca.* Marinimicrobia, SAR324, and the Marine Group II of the phylum Euryarchaeota (MGII). Within this first phase, the most ancient clade was the SAR202 (2479 My, 95% CI = 2465-2492 My), whose diversification took place near before the GOE (Fig. 2). The diversification of SAR202 before the rise of oxygen in the atmosphere suggests that this group emerged during an oxygen oasis proposed to have existed in pre-GOE Earth[24–26]. The ancient pre-GOE origin of SAR202 is consistent with a recent study that proposed that this clade played a role in the shift of the redox state of the atmosphere during the GOE by partially metabolizing organic matter through a flavin dependent Baeyer–Villiger monooxygenase, thereby enhancing the burial of organic matter and contributing to the net accumulation of oxygen in the atmosphere[27,28]. After

123 the GOE, we detected the diversification of aerobic *Ca.* Marinimicrobia (2196 My, 95% CI =
124 2173-2219 My), the SAR324 clade (1686 My, 95% CI = 1658-1715 My), and the MGII clade
125 (1184 My, 95% CI = 1166-1202 My) (Fig. 2). Although these ancient clades may have first
126 diversified in an oxic environment, the abrupt first increase of oxygen during the GOE was
127 followed by a relatively rapid drop in ocean and atmosphere oxygen levels[25,29,30]. It is therefore
128 likely that these clades diversified in the microaerophilic and variable oxygen conditions that
129 prevailed during this period[20–22]. Indeed, the oxygen landscape in which these marine clades first
130 diversified is consistent with their current physiology. There groups are capable of using oxygen
131 as terminal electron acceptor however, they are prevalent in modern marine oxygen minimum
132 (OMZs), where they use a wide range of alternative electron acceptors (e.g., nitrate and sulfate)[31–
133 33]. The facultative aerobic or microaerophilic metabolism in these clades is therefore likely a
134 vestige of the low oxygen environment of most of the Proterozoic Eon, and in this way OMZs can
135 be considered to be modern-day refugia of these ancient ocean conditions. Of the clades that
136 diversified as part of this early phase, MGII and SAR324 show the youngest colonization dates,
137 but we suspect that this may be due to the notably long branches that lead to the crown nodes of
138 these lineages. These long branches are likely caused by the absence of basal-branching members
139 of these clades ─ either due to extinction events or under-sampling of rare lineages in the available
140 genome collection ─ that would have increased the age of these lineages if present.
141
142 The second phase of diversification can be traced back to the time around the Neoproterozoic
143 Oxygenation Event (POE) that occurred 800-540 My[30,34], and included the clades SAR116 (959
144 My, 95% CI = 945-973 My), SAR11 (725 My, 95% CI = 715-734 My), SAR86 (503 My, 95% CI
145 = 497-509 My), SAR92 (430 My, 95% CI = 423-437 My), and Roseobacter (332 My, 95% CI =

146 323-340 My) (Fig. 2). The relative late appearance of these heterotrophic lineages abundant in the
147 open ocean today was likely due to the low productivity and oxygen concentrations in both shallow
148 and deep waters that prevailed in the Mid-Proterozoic (1800-800 My), a period known as the
149 "boring billion"[20,25,29,35–38]. The diversification of these clades may be indirectly associated with
150 the tectonic activity and a Snowball event before the NOE[35,39,40], which increased the availability
151 of terrestrial inorganic nutrients[35], and is also coincident with the widespread diversification of
152 large eukaryotic algae during the Neoproterozoic[35,39,41–43]. It is therefore plausible that an increase
153 in nutrients as well as the broad diversification of eukaryotic plankton enhanced the mobility of
154 organic and inorganic nutrients beyond the coastal areas, and increased the burial of organic matter
155 that consequently led to an increment in atmospheric oxygen concentrations[39,44]. The scenario in
156 which heterotrophic marine clades diversified in part as a consequence of the new niches built by
157 marine eukaryotes has been previously proposed to have driven the diversification of the
158 Roseobacter clade[15,45]. Our results support this phenomenon and suggest that the interaction with
159 marine Eukaryotes broadly influenced the diversification of several other heterotrophic lineages.
160 We also report the diversification of the chemolithoautotroph archaeal lineage MGI into the ocean
161 during this second phase (678 My, 95% CI = 668-688 My) (Fig 2), which is comparable with the
162 age reported by another independent study[10]. This is consistent with an increase in the oxygen
163 concentrations of the ocean during this period[25], a necessary requisite for ammonia oxidation.
164 Moreover, the widespread sulfidic conditions that have been proposed to have prevailed in the
165 Mid-Proterozoic ocean likely limited the availability of redox-sensitive metals like Cupper,
166 necessary for ammonia monooxygenases[35,46]. It is therefore possible that a low concentration of
167 oxygen and limited inorganic nutrient availability before the NOE were limiting factors that
168 delayed the colonization of AOA into the ocean. Similar to what we observed in MGII and

169 SAR324, the Roseobacter clade shows a long branch leading to the crown node (Fig. 1), suggesting

170 that the diversification of this clade occurred earlier.

171

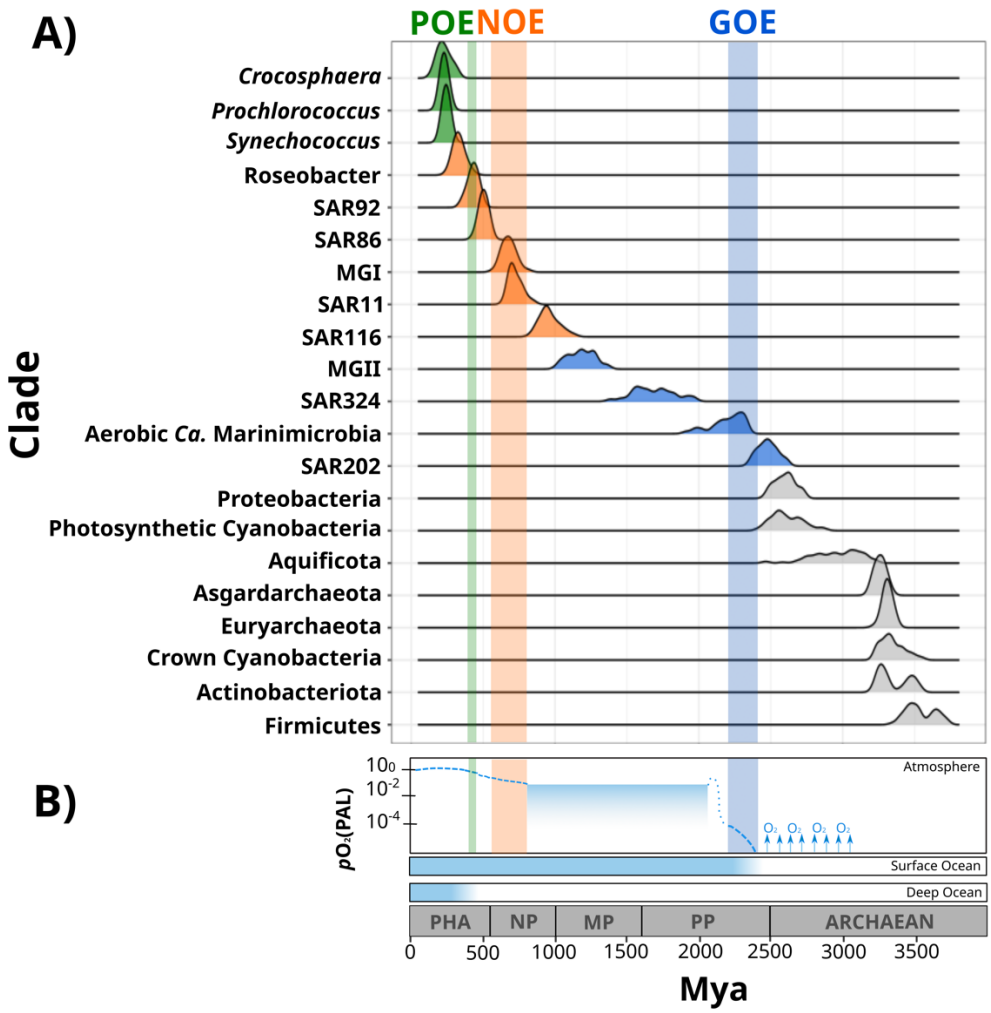

172

173 **Figure 2. Dates of the diversification of marine microbial clades and their relationship with**
174 **the redox history of Earth's atmosphere, surface ocean, and deep ocean.** A) Ridges represent
175 the distribution of 100 Bayesian dates estimated using a relaxed molecular clock and an
176 autocorrelated model (see Methods). Ridges of marine clades were colored based on their
177 diversification date: green, Late-branching Phototrophs; orange, Late-branching Clades; blue,
178 Early-branching Clades. The timing of the diversification of major bacterial and archaeal
179 superphyla is represented with gray ridges. B) Oxygenation events and redox changes across
180 Earth's history. Panel adapted from previous work[30]. Abbreviations: POE, Paleozoic Oxidation
181 Event; NOE, Neoproterozoic Oxidation Event; GOE, Great Oxidation Event; Pha, Paleozoic; NP,
182 Neoproterozoic; MP: Mesoproterozoic; PP: Paleoproterozoic.

183 The most recent and last phase of microbial diversification led to the appearance of late-branching
184 phototrophs of the genera *Synechococcus* (243 My, 95% CI = 238-247 My), *Prochlorococcus* (230
185 My, 95% CI = 225-234 My), and the nitrogen-fixer *Crocosphaera* (228 My, 95% CI = 218-237
186 My). Our results agree with an independent study that points to a relatively late evolution of the
187 marine cyanobacterial clades *Prochlorococcus* and *Synechococcus*[13]. Picocyanobacteria and
188 *Crocosphaera* are essential components of phytoplanktonic communities in the modern open
189 ocean due to their large contribution to carbon and nitrogen fixation, respectively[47–49]. For
190 example, the nitrogen fixation activities of *C. watsonii* in the open ocean today support the
191 demands of nitrogen-starved microbial food webs found in oligotrophic waters[50]. The relatively
192 late diversification of these lineages suggests that the oligotrophic open ocean is a relatively new
193 ecosystem. Moreover, the oligotrophic ocean today is characterized by the rapid turnover of
194 nutrients that depends on the efficient mobilization of essential elements through the ocean[51]. Due
195 to its distance from terrestrial nutrient inputs, productivity in the open ocean is therefore dependent
196 on local nitrogen fixation, which was likely enhanced after the widespread oxygenation of the
197 ocean that made Molybdenum widely available due to its high solubility in oxic seawater[52–54].
198 Such widespread oxygenation was registered 430-390 My in an event referred to here as the
199 Paleozoic Oxidation Event[55–58] (POE, Fig. 2). The increase of oxygen to present-day levels in the
200 atmosphere and the ocean was the result of an increment of the burial of organic carbon in
201 sedimentary rocks due to the diversification of the earliest land plants[25,57,59], which has been also
202 associated with increased phosphorus weathering rates[57,60], global impacts on the global element
203 cycles[61], and an increase in overall ocean productivity[59]. The late diversification of oligotrophic-
204 specialized clades after the POE therefore suggests that the establishment of the oligotrophic open

205 ocean as we know it today would only have been possible once modern oxygen concentrations and
206 biogeochemical dynamics were reached[25,51].
207
208 In order to shed further light on the drivers of the colonization of the ocean, we investigated
209 whether the diversification of marine microbial clades was linked to the acquisition of novel
210 metabolic capabilities. Due to the timing of diversification events during the phases described
211 previously, we classified the marine clades as Early-branching Clades, Late-branching Clades, and
212 Late-branching Phototrophs based on their diversification timing (Fig. 2). To identify the
213 enrichment of gene functions at the base of each marine clade (Fig. 1), we performed a stochastic
214 mapping analysis on each of the 112,248 protein families encoded in our genome dataset. We
215 compared our results with a null hypothesis distribution in which a constant rate model was
216 implemented unconditionally of observed data (see Methods). Statistical comparisons of the
217 stochastic and the null distribution show that overall, each diversification phase was associated
218 with the enrichment of specific functional categories that were consistent with the geochemical
219 context of their diversification (Fig. 3 and 4). For example, Early-branching Clades (EBC) gained
220 a disproportionate number of genes involved in DNA repair, recombination, and glutathione
221 metabolism, consistent with the hypothesis that the GOE led to a rise in reactive oxygen species
222 that cause DNA damage[62–64]. Moreover, the EBC were enriched in proteins involved in ancient
223 aerobic pathways, like oxidative phosphorylation and TCA cycle (Fig. 3), as well as genes
224 implicated in the degradation of fatty acids under aerobic conditions, for example the enzyme
225 alkane 1-monooxygenase in MGII (Supplemental File 6). We also detected genes for the
226 adaptation to marine environments, for instance genes for the anabolism of taurine (e.g., cysteine
227 dioxygenase in MGII, Supplemental File 6), an osmoprotectant commonly found in marine

228 bacteria[65]. Our findings suggest that the diversification of EBC in the ocean was linked to the
229 evolution of aerobic metabolism, the acquisition of metabolic capabilities to exploit the newly
230 created niches that followed the increase of oxygen, and the expansion of genes involved in the
231 tolerance to oxidative and salinity stress.
232
233

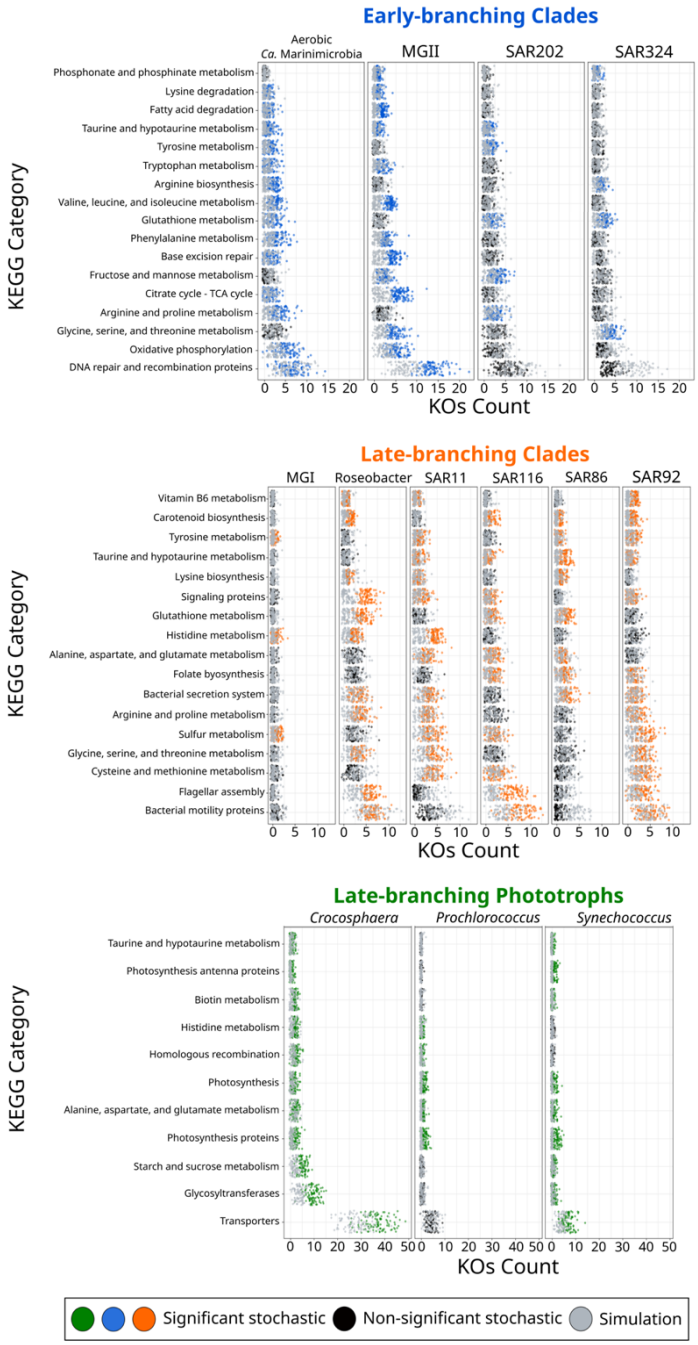

Figure 3. KEGG categories enriched at the crown node of each marine microbial clade. Clades were classified based on their diversification timing shown in Fig. 2. Enriched categories were identified by statistically comparing a stochastic mapping distribution with an all-rates-different model vs a null distribution with a constant rate model without conditioning on the presence/absence data at the tips. Each dot represents one replicate (See Methods). X-axis represents the number of KOs gained at each crown node for each KEGG category. Stochastic mapping and null distributions were sorted for visualization purposes. The complete list of enriched KEGGs is shown in Supplemental File 7.

243 The emergence of Late-branching Clades (LBC; Fig. 3 and 4), whose diversification occurred
244 around the time of the NOE and the initial diversification of eukaryotic algae[66], was characterized
245 by the enrichment of substantially different gene repertories compared to EBC (Fig. 3). For
246 instance, the heterotrophic lineages Roseobacter, SAR116, and SAR92 show an enrichment of
247 flagellar assembly and motility genes (Fig. 3), including genes for flagellar biosynthesis, flagellin,
248 and the flagellar basal-body assembly (Supplemental File 6). Motile marine heterotrophs like
249 Roseobacter species have been associated with the marine phycosphere, a region surrounding
250 individual phytoplankton cells releasing carbon-rich nutrients[67,68]. Although the phycosphere can
251 also be found in prokaryotic phytoplankton[67], given the late diversification of abundant marine
252 prokaryotic phytoplankton (Fig. 2 and 4), it is plausible that the emergence of these clades was
253 closely related to the establishment of ecological proximity with large eukaryotic algae, as
254 suggested by our Bayesian estimates (Fig. 2 and 4). The potential diversification of heterotrophic
255 LBC due to their ecological proximity with eukaryotic algae is further supported by the enrichment
256 of genes involved in vitamin B6 metabolism and folate biosynthesis, which are key nutrients
257 involved in phytoplankton-bacteria interactions[67,69]. LBC were also enriched in genes for the
258 catabolism of taurine (e.g., taurine transport system permease in SAR11 and a taurine dioxygenase
259 in SAR86 and SAR92), suggesting that LBC gained metabolic capabilities to utilize the taurine
260 produced by other organisms as substrate[70], instead of producing it as osmoprotectant.
261 Furthermore, we identified the enrichment of genes involved in carotenoid biosynthesis, including
262 spheroidene monooxygenase, carotenoid 1,2-hydratase, beta-carotene hydroxylase, and lycopene
263 beta-cyclase (Supplemental File 6). The production of carotenoids is consistent with their use in
264 proteorhodopsin, a light driven proton pump that is a hallmark feature of most marine heterotrophic
265 bacteria, in particular those that inhabit energy-depleted areas of the ocean[71]. The enrichment of

genes potentially involved in bacteria-phytoplankton interactions suggest that the diversification of marine clades during the NOE was intimately linked to the establishment of ecological relationships with eukaryotes to exchange nutrients.

Late-branching phototrophs that diversified around the time of the POE (LBP; Fig. 2), showed the enrichment of transporters in *Crocosphaera* and *Synechococcus* (Fig. 3). In particular, the diversification of *Crocosphaera* was characterized by the acquisition of transporters for inorganic nutrients like cobalt, nickel, iron, phosphonate, phosphate, ammonium, and magnesium, along with organic nutrients including amino acids and polysaccharides (Supplemental File 6). The acquisition of a wide diversity of transporters by the *Crocosphaera* is consistent with their boom-and-bust lifestyle seen in the oligotrophic open ocean today[50,72], which requires a rapid and efficient use of the scarce nutrients available. We also identified genes for osmotic pressure tolerance, for example a Ca-activated chloride channel homolog, a magnesium exporter, and a fluoride exporter (Supplemental File 6). This finding suggests that *Crocosphaera* might have diversified from a non-marine group into the ocean. In contrast, our results show that *Synechococcus* only acquired transporters for inorganic nutrients (e.g., iron and sulfate, Supplemental File 6), whereas *Prochlorococcus* did not show an enrichment of transporters (Supplemental File 6). The absence of salt-tolerance related genes suggests that the ancestor of these Picocyanobacterial clades inhabited a low-nutrient marine habitat. Similar to LBC, we identified the enrichment of taurine metabolism genes in *Crocosphaera* and *Synechococcus*, suggesting that its use as osmoprotectant and potential substrate is widespread among planktonic microorganisms[70]. *Prochlorococcus* exhibits enrichment in fewer categories than the rest of phototrophic clades diversifying during the same period, consistent with the streamlined nature of

289 genomes from this lineage[73]. The genes acquired by this lineage are involved in photosynthesis,
290 which supports previous findings that the diversification of this clade was accompanied by changes
291 in the photosynthetic apparatus compared with *Synechococcus*, its sister group[74]. Overall, the
292 diversification of LBP was marked by the capacity to thrive in the oligotrophic ocean by exploiting
293 organic and inorganic nutrients and modifying the photosynthetic apparatus as observed in
294 *Crocosphaera* and *Synechococcus*, and *Prochlorococcus,* respectively.
295
296 The contemporary ocean is dominated by abundant clades of bacteria and archaea that drive global
297 biogeochemical cycles and play a central role in shaping the redox state of the planet. Despite their
298 importance, the timing, and the geological landscape at which these clades colonized the ocean
299 have remained unclear due to a combination of the inherent difficulties of studying biological
300 events that occurred in deep time and the lack of a fossil record for microbial life. Here we present
301 a comprehensive timeline for the colonization of the ocean by abundant marine clades and reveal
302 that major oxygenation events in Earth's history played critical roles in creating new niches for
303 microbial diversification. These colonization events subsequently led to the establishment of the
304 biogeochemical cycles that govern the environmental stability of our planet today. Our study
305 allowed us to reconstruct a framework that links major geological and biological events to the
306 emergence of microbial lineages that dominate the contemporary ocean (Fig. 4). This provides key
307 foundational knowledge for understanding ongoing anthropogenic changes in the ocean.
308 Importantly, climate change is predicted to lead to an expansion of both oxygen minimum zones,
309 which represent refugia dating back to the mid-Proterozoic ocean, and oligotrophic surface waters,
310 which represent ecosystems that have emerged relatively recently in the Phanerozoic. Thus, the
311 impacts of current global change can manifest similarly in ecosystems that have emerged at

dramatically different periods of Earth's history. Knowledge of how and under what geochemical conditions dominant microbial constituents first diversified provides critical context for understanding the impact of drastic climatic changes on the marine biome more broadly and will help to clarify how continuing ecological shifts will impact marine biogeochemical cycles.

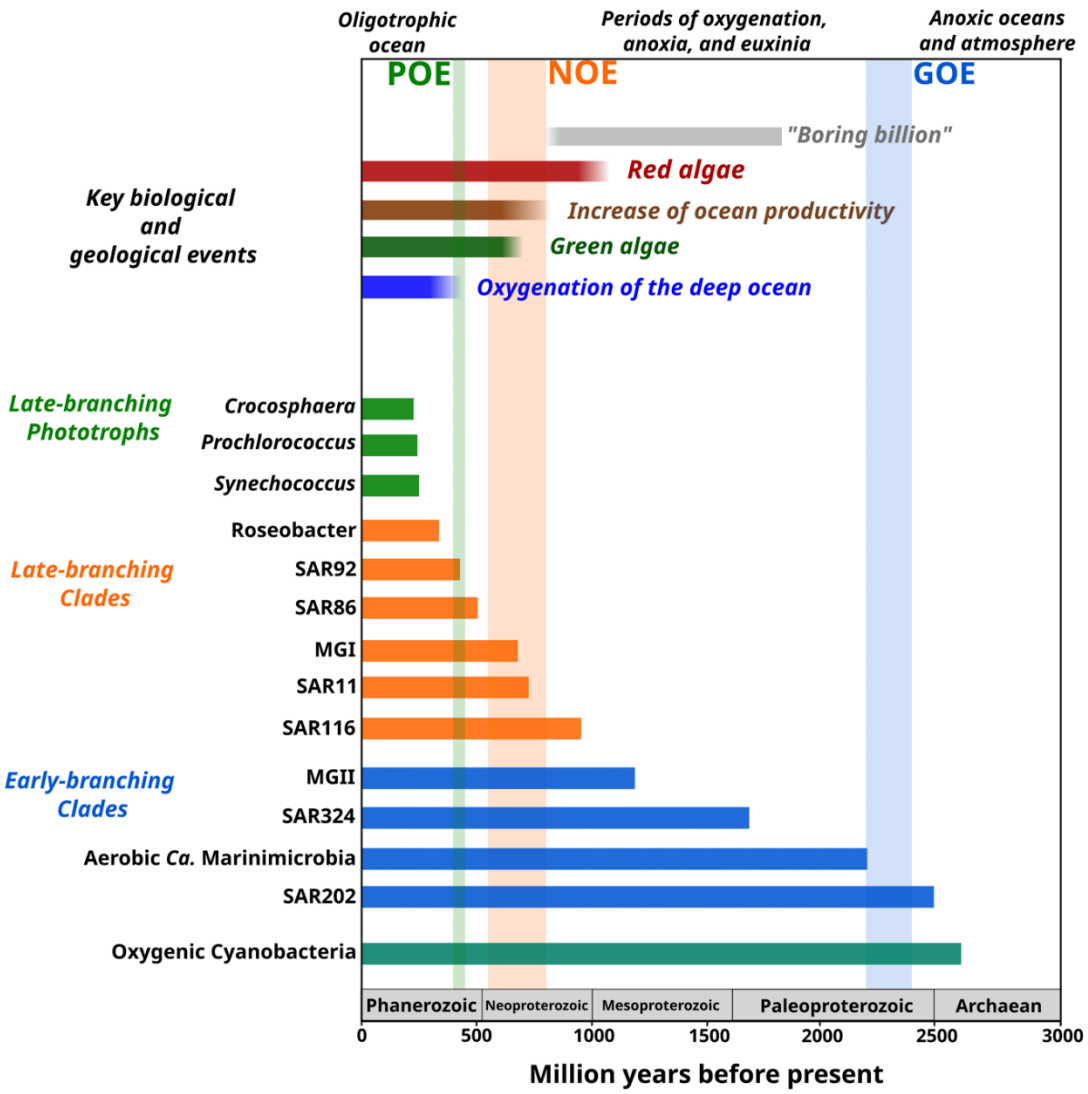

Figure 4. Link between the timing of the diversification of the main marine microbial clades and major geological and biological events. The timing of the geological and biological events potentially involved in the diversification of marine clades is based on previously published data: "Boring billion"[96], red algae fossils[97], increased of ocean productivity[34], green algae fossils[98], oxygenation of the deep ocean[57]. The length of each bar represents the estimated age for marine clades according to Bayesian estimates. The timing of the main oxygenation events is based on previous work[30].

MATERIAL AND METHODS

Genomes sampling and phylogenetic reconstruction

In order to obtain a comprehensive understanding of the diversification of the main marine planktonic clades, we built a multi-domain phylogenetic tree that included a broad diversity of bacterial and archaeal genomes. We compiled a balanced genome dataset subsampled from the Genome Taxonomy Database[75] (GTDB, v95), including marine representatives. In addition, we improved the representation of marine genomes by subsampling genomes from the GORG database[76], which includes a wide range of genomes derived from single-cell sequencing, and adding several *Thermoarchaeota* genomes available on the JGI[77]. We discarded genomes belonging to the DPANN superphylum due to the uncertainty of their placement within the archaea[16]. The list of genomes used is reported in Supplemental File 1.

We reconstructed a phylogenetic tree through the MarkerFinder pipeline developed previously[16], which resulted in an alignment of 27 ribosomal genes and three RNA polymerase genes (RNAP)[16]. The MarkerFinder pipeline consists of 1) the identification of ribosomal and RNAP genes using HMMER v 3.2.1 with the reported model-specific cutoffs[78], 2) alignment with ClustalOmega[78,79], and 3) concatenation of individual alignments. The resulting concatenated alignment was trimmed using trimAl[80] with the option -gt 0.1. Phylogenetic tree inference was carried out with IQ-TREE v1.6.12[81] with the options -wbt, -bb 1000[82], -m LG+R10 (substitution model previously selected with the option -m MFP according to the Bayesian Information Criterion[83]), and --runs 5 to select the tree with the highest likelihood. The tree with the highest likelihood was manually inspected to discard the presence of topological inconsistencies and artifacts on iTOL[84] (Fig .1). The raw phylogenetic tree is presented in Supplemental File 2.

347 *Assessment of Quality Tree*

348 Due to the key importance of tree quality for the tree-dependent analysis performed in our study,
349 we assessed the congruence of our prokaryotic ToL through the Tree Certainty metric (TC)[16,85],
350 which has recently been shown to be a more accurate estimate for phylogenetic congruence that
351 the traditional bootstrap. Our estimate based on 1,000 replicate trees (TC = 0.91) indicates high
352 congruence in our phylogeny, indicating that the phylogenetic signal across our concatenated
353 alignment of marker genes is consistent. We also evaluated whether the topology of our ToL is in
354 agreement with a high-quality prokaryotic ToL reported previously[16]. In general, we observed
355 consistency in the placement of the all the phyla, as well as the bacterial superphyla (Terrabacteria
356 and Gracilicutes) between both trees, except for the sisterhood of Actinobacteriota and
357 Armatimonadota, which differs from the sisterhood of Actinobacteriota and Firmicutes in the
358 reference tree[16]. Despite this discrepancy, we do not expect that it will substantially impact the
359 results of the current study because none of the marine clades are within this region of the tree.

360

361 *Estimating the age of the crown node of bacterial and archaeal marine clades*

362 In order to investigate the timing of the diversification of marine planktonic clades of interest, the
363 phylogenetic tree obtained previously was used to perform a molecular dating analysis of the
364 crown nodes leading to the diversification of the main marine microbial clades. Our analysis was
365 performed through Phylobayes v4.1c[86] with the program pb on four independent chains. For each
366 chain, the input consisted in the phylogenetic tree, the amino acids alignment, the calibrations, and
367 an autocorrelated relaxed log normal model (-ln)[87] with the default molecular evolution model.
368 Convergence was tested every 5000 cycles using the program tracecomp with a burn-in of 250
369 cycles and sampling every 2 cycles. After 100,000 cycles, our chains reached convergence in 8

370 out of 12 parameters (Supplemental File 3). In order to assess the uncertainty derived from the
371 parameters that did not reach convergence, we estimated the divergence ages for each of our four
372 chains using the last 1000 cycles and a range of 10 cycles to have a sample of 100 age estimates
373 using the program readdiv (Supplemental File 4). We report the confidence intervals and the
374 median age of 100 replicates of chain three throughout the manuscript.
375
376 To determine the impact of our priors (Fig. 1 and Table 1) on the age estimates of the calibrated
377 nodes in our tree and assess the suitability of the ages used as priors for our analyses, we ran an
378 independent MCMC chain without the amino acid alignment using the option -root on Phylobayes.
379 Our prior-only analysis yielded a posterior age falling within the maximum and minimum priors
380 used for the crown group of archaea and bacteria. For the internal calibrated nodes, we observed
381 posterior estimates consistent with the priors used for each case except for aerobic ammonia
382 oxidizing archaea (Supplemental File 5 and 6). Overall, this result suggests that the calibrations
383 used as priors were adequate for our analyses.
384
385 To evaluate the reproducibility of our Bayesian molecular dating analysis, we applied a second
386 independent approach based on Penalized Likelihood (PL) using the TreePL[88] program on 1000
387 replicate bootstrap trees that had fixed topology but varying branch lengths. Replicate trees were
388 generated with the program bsBranchLenghts available on RAxML v8.2.12[89]. For each replicate
389 run, we initially used the option "prime" to identify the optimization parameters and applied the
390 parameters "through" to continue iterations until convergence in the parameters of each of the
391 1000 runs. Moreover, we estimated the optional smoothing value for each replicate tree and ran
392 cross-validation with the options "cv" and "randomcv"[88]. The divergence times resulting from the

393 1000 bootstrap trees were used to assess the age variation for each node of interest (Supplemental
394 File 4).
395
396 *Comparison among PhyloBayes chains and between TreePL age estimates*
397 Although some Bayesian parameters did not reach convergence after 100,000 cycles
398 (Supplemental File 3), the estimated ages resulting from our four independent chains were similar
399 when compared to each other (Supplemental File 4). Moreover, our Bayesian and Penalized
400 likelihood approaches showed similar divergence times, strengthening the conclusions of our
401 study. We only observed notable discrepancies between these approaches in Photosynthetic
402 Cyanobacteria (PL showing more recent divergence during the GOE), and the marine
403 Picocyanobacteria *Synechococcus* and *Prochlorococcus* (PL showing more ancient divergence
404 during the POE). Despite these discrepancies, the differences observed between both approaches
405 do not alter our main conclusions regarding the phases during which these major marine clades
406 diversified.
407
408 *Comparing Bayesian diversification estimates with previous studies*
409 Two estimated divergence times shown in our study disagree with previously published analyses.
410 Firstly, a recent molecular dating estimate suggested that the transition of AOA-Archaea from
411 terrestrial environments into marine reals occurred before the NOE[11] during a period known as the
412 "boring million" characterized by low productivity and minimum oxygen concentrations in the
413 atmosphere (0.1% the present levels)[20,25,29,35]. Our estimates point to a later diversification of this
414 lineage during or after the NOE (678 Mya, 95% CI = 668-688 Mya) (Fig. 2), which is comparable
415 with the age reported by another independent study[10]. Secondly, another study reported the origin

416 of the Picocyanobacterial clade *Prochlorococcus* to be 800 My, before the Snowball Earth period
417 registered during the Cryogen[12]. However, our results agree with another independent study that
418 points to a relatively late evolution of *Prochlorococcus*[13].
419
420 *Orthologous groups detection, stochastic mapping, and functional annotation*
421 To investigate the genomic novelties associated with the diversification of the marine microbial
422 lineages considered in our study, we identified enriched KEGG categories in the crown node of
423 each clade. First, we predicted protein orthologous groups with ProteinOrtho v6[90] using the option
424 "lastp" and protein files downloaded from the GTDB, GORG, and JGI databases. Furthermore,
425 we performed a functional annotation using the KEGG database[91–93] through HMMER3 with an
426 e-value of 10^{-5} on all proteins. Proteins with multiple annotations were filtered to keep the best-
427 scored annotation, and we predicted the function of each protein orthologous group by using the
428 Majority Rule Principle. The presence/absence matrix resulting from the identification of
429 orthologous groups was used together with the phylogenetic tree utilized for molecular dating to
430 perform 100 replicate stochastic mapping analyses on each orthologous group with the
431 make.simmap function implemented on Phytools[94,95] with the model "all-rates-different" (ARD).
432 To evaluate evidence of enrichment of KEGG categories, we created a null distribution for each
433 protein cluster by simulating under the transition matrix estimated from our stochastic mapping
434 analysis using the function sim.history, but without conditioning on the presence/absence data at
435 the tips (i.e. simulating a constant rate null distribution of transitions across the tree). Since some
436 of the protein clusters show a low exchange rate (identified because one of the rows in the Q-
437 matrix was equal to zero), we manually changed the exchange rate from zero to 0.00001. For each
438 distribution, we estimated the number of genes gained for each KEGG category at the crown node

of the marine clades. Clusters without a known annotation on the KEGG database were discarded. The resulting KEGG categories distributions for our stochastic mapping and null analyses were statistically compared using a one-tailed Wilcox test (α=0.01, N= 100 for each distribution). KEGG categories showing statistically more gains in our stochastic mapping distribution were considered enriched (Supplemental File 7).

ACKNOWLEDGMENTS

We acknowledge the use of the Virginia Tech Advanced Research Computing Center for bioinformatic analyses performed in this study. This investigation was supported by grants from the Institute for Critical Technology and Applied Science and the National Science Foundation (IIBR-2141862), and a Simons Early Career Award in Marine Microbial Ecology and Evolution to F.O.A. We kindly thank members of the Aylward Lab for their insightful comments on an earlier version of this manuscript.

AUTHORS CONTRIBUTIONS

Conceived and designed this work: CAMG, UJC, and FOA. Wrote the manuscript: CAMG, UJC, and FOA.

MATERIALS AND CORRESPONDACE

Frank O. Aylward; faylward@vt.edu

Carolina A. Martinez-Gutierrez; cmartinez@vt.edu

SUPPLEMENTAL MATERIALS

Supplemental File 1. Genomes dataset used for the molecular dating of the main marine microbial clades.

Supplemental File 2. Raw maximum likelihood phylogenetic tree used for molecular dating and stochastic mapping analyses.

Supplemental File 3. Assessment of parameters convergence of four independent chains used for Bayesian molecular dating analyses. Relative difference <0.3 is shown in bold letters and denotes parameters that reached convergence after 100,000 cycles using a burn-in of 250 and sampling every two cycles.

Supplemental File 4. Comparison of the age distribution of marine microbial clades and its relationship with the main Earth oxygenation events using a Bayesian and a Penalized Likelihood approach for molecular dating. Ridges represent the age of 100 and 1000 replicate age estimates for each Bayesian independent chains and Penalized Likelihood analyses, respectively (see Methods).

Supplemental File 5. Estimated ages for calibrated nodes showing their suitability as priors for Bayesian molecular dating. Values resulted from running an independent chain on the temporal calibrations without sequence data (-root option on Phylobayes). Bars represent the standard error of the cycles tested.

Supplemental File 6. KOs gained at the crown node of each marine microbial clade. A KO was considered as gained when found in 51 out of 100 stochastic mapping replicates.

Supplemental File 7. KEGG categories enriched at the crown node of each marine microbial clade. Clades were classified based on the diversification timing shown in Fig. 2. Enriched categories were identified by statistically comparing a stochastic mapping distribution with an all-rates-different vs a null distribution with a constant rate model without conditioning on the presence/absence data at the tips. Each dot represents one replicate (See Methods). X-axis represents the number of KOs gained at each crown node for each KEGG category. Stochastic mapping and null distributions were sorted for visualization purposes.

REFERENCES

1. Falkowski, P. G., Barber, R. T. & Smetacek, V., V. Biogeochemical Controls and Feedbacks on Ocean Primary Production. *Science* **281**, 200–207 (1998).
2. Falkowski, P. G., Fenchel, T. & Delong, E. F. The microbial engines that drive Earth's biogeochemical cycles. *Science* **320**, 1034–1039 (2008).
3. Field, C. B., Behrenfeld, M. J., Randerson, J. T. & Falkowski, P. Primary production of the biosphere: integrating terrestrial and oceanic components. *Science* **281**, 237–240 (1998).
4. Mason, O. U. *et al.* Prokaryotic diversity, distribution, and insights into their role in biogeochemical cycling in marine basalts. *ISME J.* **3**, 231–242 (2009).
5. Brown, M. V., Ostrowski, M., Grzymski, J. J. & Lauro, F. M. A trait based perspective on the biogeography of common and abundant marine bacterioplankton clades. *Mar. Genomics* **15**, 17–28 (2014).
6. Ducklow, H. W. & Doney, S. C. What Is the Metabolic State of the Oligotrophic Ocean? A Debate. *Annual Review of Marine Science* vol. 5 525–533 Preprint at https://doi.org/10.1146/annurev-marine-121211-172331 (2013).
7. Zehr, J. P. & Kudela, R. M. Nitrogen cycle of the open ocean: from genes to ecosystems. *Ann. Rev. Mar. Sci.* **3**, 197–225 (2011).
8. Vila-Costa, M. *et al.* Dimethylsulfoniopropionate uptake by marine phytoplankton. *Science* **314**, 652–654 (2006).
9. Giovannoni, S. J. & Stingl, U. Molecular diversity and ecology of microbial plankton. *Nature* vol. 437 343–348 Preprint at https://doi.org/10.1038/nature04158 (2005).
10. Yang, Y. *et al.* The Evolution Pathway of Ammonia-Oxidizing Archaea Shaped by Major Geological Events. *Mol. Biol. Evol.* **38**, 3637–3648 (2021).
11. Ren, M. *et al.* Phylogenomics suggests oxygen availability as a driving force in Thaumarchaeota evolution. *ISME J.* **13**, 2150–2161 (2019).
12. Zhang, H., Sun, Y., Zeng, Q., Crowe, S. A. & Luo, H. Snowball Earth, population bottleneck and *Prochlorococcus* evolution. *Proceedings of the Royal Society B: Biological Sciences* vol. 288 Preprint at https://doi.org/10.1098/rspb.2021.1956 (2021).
13. Sánchez-Baracaldo, P. Origin of marine planktonic cyanobacteria. *Sci. Rep.* **5**, 17418 (2015).
14. Sánchez-Baracaldo, P., Bianchini, G., Di Cesare, A., Callieri, C. & Chrismas, N. A. M. Insights Into the Evolution of Picocyanobacteria and Phycoerythrin Genes (mpeBA and

cpeBA). *Frontiers in Microbiology* vol. 10 Preprint at https://doi.org/10.3389/fmicb.2019.00045 (2019).

15. Luo, H., Csuros, M., Hughes, A. L. & Moran, M. A. Evolution of divergent life history strategies in marine alphaproteobacteria. *MBio* **4**, (2013).
16. Martinez-Gutierrez, C. A. & Aylward, F. O. Phylogenetic Signal, Congruence, and Uncertainty across Bacteria and Archaea. *Mol. Biol. Evol.* **38**, 5514–5527 (2021).
17. Coleman, G. A. *et al.* A rooted phylogeny resolves early bacterial evolution. *Science* **372**, (2021).
18. Valley, J. W. *et al.* Hadean age for a post-magma-ocean zircon confirmed by atom-probe tomography. *Nature Geoscience* vol. 7 219–223 Preprint at https://doi.org/10.1038/ngeo2075 (2014).
19. Ueno, Y., Yamada, K., Yoshida, N., Maruyama, S. & Isozaki, Y. Evidence from fluid inclusions for microbial methanogenesis in the early Archaean era. *Nature* **440**, 516–519 (2006).
20. Holland, H. D. The oxygenation of the atmosphere and oceans. *Philosophical Transactions of the Royal Society B: Biological Sciences* vol. 361 903–915 Preprint at https://doi.org/10.1098/rstb.2006.1838 (2006).
21. Holland, H. D. Volcanic gases, black smokers, and the great oxidation event. *Geochimica et Cosmochimica Acta* vol. 66 3811–3826 Preprint at https://doi.org/10.1016/s0016-7037(02)00950-x (2002).
22. Bekker, A. *et al.* Dating the rise of atmospheric oxygen. *Nature* vol. 427 117–120 Preprint at https://doi.org/10.1038/nature02260 (2004).
23. Ward, L. M., Kirschvink, J. L. & Fischer, W. W. Timescales of Oxygenation Following the Evolution of Oxygenic Photosynthesis. *Orig. Life Evol. Biosph.* **46**, 51–65 (2016).
24. Ossa Ossa, F. *et al.* Limited oxygen production in the Mesoarchean ocean. *Proc. Natl. Acad. Sci. U. S. A.* **116**, 6647–6652 (2019).
25. Reinhard, C. T. & Planavsky, N. J. The History of Ocean Oxygenation. *Ann. Rev. Mar. Sci.* **14**, 331–353 (2022).
26. Anbar, A. D. *et al.* A whiff of oxygen before the great oxidation event? *Science* **317**, 1903–1906 (2007).
27. Landry, Z., Swan, B. K., Herndl, G. J., Stepanauskas, R. & Giovannoni, S. J. SAR202

Genomes from the Dark Ocean Predict Pathways for the Oxidation of Recalcitrant Dissolved Organic Matter. *MBio* **8**, (2017).

28. Shang, H., Rothman, D. H. & Fournier, G. P. Oxidative metabolisms catalyzed Earth's oxygenation. *Nature Communications* vol. 13 Preprint at https://doi.org/10.1038/s41467-022-28996-0 (2022).
29. Hodgskiss, M. S. W., Crockford, P. W., Peng, Y., Wing, B. A. & Horner, T. J. A productivity collapse to end Earth's Great Oxidation. *Proceedings of the National Academy of Sciences* vol. 116 17207–17212 Preprint at https://doi.org/10.1073/pnas.1900325116 (2019).
30. Alcott, L. J., Mills, B. J. W. & Poulton, S. W. Stepwise Earth oxygenation is an inherent property of global biogeochemical cycling. *Science* **366**, 1333–1337 (2019).
31. Thrash, J. C. *et al.* Metabolic roles of uncultivated bacterioplankton lineages in the northern Gulf of Mexico 'Dead Zone'. Preprint at https://doi.org/10.1101/095471.
32. Pajares, S., Varona-Cordero, F. & Hernández-Becerril, D. U. Spatial Distribution Patterns of Bacterioplankton in the Oxygen Minimum Zone of the Tropical Mexican Pacific. *Microb. Ecol.* **80**, 519–536 (2020).
33. Sheik, C. S., Jain, S. & Dick, G. J. Metabolic flexibility of enigmatic SAR324 revealed through metagenomics and metatranscriptomics. *Environmental Microbiology* vol. 16 304–317 Preprint at https://doi.org/10.1111/1462-2920.12165 (2014).
34. Och, L. M. & Shields-Zhou, G. A. The Neoproterozoic oxygenation event: Environmental perturbations and biogeochemical cycling. *Earth-Science Reviews* vol. 110 26–57 Preprint at https://doi.org/10.1016/j.earscirev.2011.09.004 (2012).
35. Anbar, A. D. & Knoll, A. H. Proterozoic ocean chemistry and evolution: a bioinorganic bridge? *Science* **297**, 1137–1142 (2002).
36. Tang, D., Shi, X., Wang, X. & Jiang, G. Extremely low oxygen concentration in mid-Proterozoic shallow seawaters. *Precambrian Research* vol. 276 145–157 Preprint at https://doi.org/10.1016/j.precamres.2016.02.005 (2016).
37. Crockford, P. W. *et al.* Triple oxygen isotope evidence for limited mid-Proterozoic primary productivity. *Nature* vol. 559 613–616 Preprint at https://doi.org/10.1038/s41586-018-0349-y (2018).
38. Planavsky, N. J. *et al.* Earth history. Low mid-Proterozoic atmospheric oxygen levels and the delayed rise of animals. *Science* **346**, 635–638 (2014).

39. Shields-Zhou, G. & Och, L. The case for a Neoproterozoic Oxygenation Event: Geochemical evidence and biological consequences. *GSA Today* vol. 21 4–11 Preprint at https://doi.org/10.1130/gsatg102a.1 (2011).
40. Hoffman, P. F., Kaufman, A. J., Halverson, G. P. & Schrag, D. P. A Neoproterozoic Snowball Earth. *Science* vol. 281 1342–1346 Preprint at https://doi.org/10.1126/science.281.5381.1342 (1998).
41. Butterfield, N. J. Paleobiology of the late Mesoproterozoic (ca. 1200 Ma) Hunting Formation, Somerset Island, arctic Canada. *Precambrian Research* vol. 111 235–256 Preprint at https://doi.org/10.1016/s0301-9268(01)00162-0 (2001).
42. Vidal, G. & Moczydłowska-Vidal, M. Biodiversity, speciation, and extinction trends of Proterozoic and Cambrian phytoplankton. *Paleobiology* vol. 23 230–246 Preprint at https://doi.org/10.1017/s0094837300016808 (1997).
43. Porter, S. M. The fossil record of early eukaryotic diversification. *The Paleontological Society Papers* vol. 10 35–50 Preprint at https://doi.org/10.1017/s1089332600002321 (2004).
44. Knoll, A. H., Javaux, E. J., Hewitt, D. & Cohen, P. Eukaryotic organisms in Proterozoic oceans. *Philos. Trans. R. Soc. Lond. B Biol. Sci.* **361**, 1023–1038 (2006).
45. Luo, H. & Moran, M. A. Evolutionary ecology of the marine Roseobacter clade. *Microbiol. Mol. Biol. Rev.* **78**, 573–587 (2014).
46. Hatzenpichler, R. Diversity, physiology, and niche differentiation of ammonia-oxidizing archaea. *Appl. Environ. Microbiol.* **78**, 7501–7510 (2012).
47. Scanlan, D. J. *et al.* Ecological Genomics of Marine Picocyanobacteria. *Microbiology and Molecular Biology Reviews* vol. 73 249–299 Preprint at https://doi.org/10.1128/mmbr.00035-08 (2009).
48. Flombaum, P. *et al.* Present and future global distributions of the marine Cyanobacteria *Prochlorococcus* and *Synechococcus*. *Proceedings of the National Academy of Sciences* vol. 110 9824–9829 Preprint at https://doi.org/10.1073/pnas.1307701110 (2013).
49. Montoya, J. P. *et al.* High rates of N2 fixation by unicellular diazotrophs in the oligotrophic Pacific Ocean. *Nature* **430**, 1027–1032 (2004).
50. Hewson, I. *et al.* In situ transcriptomic analysis of the globally important keystone N2-fixing taxon Crocosphaera watsonii. *ISME J.* **3**, 618–631 (2009).
51. Karl, D. M. Nutrient dynamics in the deep blue sea. *Trends Microbiol.* **10**, 410–418 (2002).

52. Scott, C. *et al.* Tracing the stepwise oxygenation of the Proterozoic ocean. *Nature* **452**, 456–459 (2008).
53. Canfield, D. E., Poulton, S. W. & Narbonne, G. M. Late-Neoproterozoic Deep-Ocean Oxygenation and the Rise of Animal Life. *Science* vol. 315 92–95 Preprint at https://doi.org/10.1126/science.1135013 (2007).
54. Wei, G.-Y. *et al.* Global marine redox evolution from the late Neoproterozoic to the early Paleozoic constrained by the integration of Mo and U isotope records. *Earth-Science Reviews* vol. 214 103506 Preprint at https://doi.org/10.1016/j.earscirev.2021.103506 (2021).
55. Sperling, E. A. *et al.* Statistical analysis of iron geochemical data suggests limited late Proterozoic oxygenation. *Nature* vol. 523 451–454 Preprint at https://doi.org/10.1038/nature14589 (2015).
56. Berner, R. A. & Raiswell, R. Burial of organic carbon and pyrite sulfur in sediments over phanerozoic time: a new theory. *Geochimica et Cosmochimica Acta* vol. 47 855–862 Preprint at https://doi.org/10.1016/0016-7037(83)90151-5 (1983).
57. Lenton, T. M. *et al.* Earliest land plants created modern levels of atmospheric oxygen. *Proc. Natl. Acad. Sci. U. S. A.* **113**, 9704–9709 (2016).
58. Tostevin, R. & Mills, B. J. W. Reconciling proxy records and models of Earth's oxygenation during the Neoproterozoic and Palaeozoic. *Interface Focus* vol. 10 20190137 Preprint at https://doi.org/10.1098/rsfs.2019.0137 (2020).
59. Planavsky, N. J. *et al.* Evolution of the structure and impact of Earth's biosphere. *Nature Reviews Earth & Environment* vol. 2 123–139 Preprint at https://doi.org/10.1038/s43017-020-00116-w (2021).
60. Bergman, N. M., (Tim) Lenton, T. M., Watson, A. J., Dynamics, B. & Biogeochemistry. *COPSE: A new model of biogeochemical cycling over Phanerozoic time*. (2004).
61. Dahl, T. W. & Arens, S. K. M. The impacts of land plant evolution on Earth's climate and oxygenation state – An interdisciplinary review. *Chemical Geology* vol. 547 119665 Preprint at https://doi.org/10.1016/j.chemgeo.2020.119665 (2020).
62. Burrows, C. J. Surviving an Oxygen Atmosphere: DNA Damage and Repair. *ACS Symp. Ser. Am. Chem. Soc.* **2009**, 147–156 (2009).
63. Masip, L., Veeravalli, K. & Georgiou, G. The many faces of glutathione in bacteria. *Antioxid. Redox Signal.* **8**, 753–762 (2006).

657 64. Khademian, M. & Imlay, J. A. How Microbes Evolved to Tolerate Oxygen. *Trends*
658 *Microbiol.* **29**, 428–440 (2021).
659 65. McParland, E. L., Alexander, H. & Johnson, W. M. The Osmolyte Ties That Bind: Genomic
660 Insights Into Synthesis and Breakdown of Organic Osmolytes in Marine Microbes. *Frontiers*
661 *in Marine Science* vol. 8 Preprint at https://doi.org/10.3389/fmars.2021.689306 (2021).
662 66. Parfrey, L. W., Lahr, D. J. G., Knoll, A. H. & Katz, L. A. Estimating the timing of early
663 eukaryotic diversification with multigene molecular clocks. *Proc. Natl. Acad. Sci. U. S. A.*
664 **108**, 13624–13629 (2011).
665 67. Seymour, J. R., Amin, S. A., Raina, J.-B. & Stocker, R. Zooming in on the phycosphere: the
666 ecological interface for phytoplankton–bacteria relationships. *Nature Microbiology* vol. 2
667 Preprint at https://doi.org/10.1038/nmicrobiol.2017.65 (2017).
668 68. Mühlenbruch, M., Grossart, H.-P., Eigemann, F. & Voss, M. Mini-review: Phytoplankton-
669 derived polysaccharides in the marine environment and their interactions with heterotrophic
670 bacteria. *Environ. Microbiol.* **20**, 2671–2685 (2018).
671 69. Croft, M. T., Lawrence, A. D., Raux-Deery, E., Warren, M. J. & Smith, A. G. Algae acquire
672 vitamin B12 through a symbiotic relationship with bacteria. *Nature* **438**, 90–93 (2005).
673 70. Clifford, E. L. *et al.* Taurine Is a Major Carbon and Energy Source for Marine Prokaryotes in
674 the North Atlantic Ocean off the Iberian Peninsula. *Microb. Ecol.* **78**, 299–312 (2019).
675 71. de la Torre, J. R. *et al.* Proteorhodopsin genes are distributed among divergent marine
676 bacterial taxa. *Proc. Natl. Acad. Sci. U. S. A.* **100**, 12830–12835 (2003).
677 72. Wilson, S. T. *et al.* Coordinated regulation of growth, activity and transcription in natural
678 populations of the unicellular nitrogen-fixing cyanobacterium Crocosphaera. *Nat Microbiol*
679 **2**, 17118 (2017).
680 73. Partensky, F. & Garczarek, L. Prochlorococcus: advantages and limits of minimalism. *Ann.*
681 *Rev. Mar. Sci.* **2**, 305–331 (2010).
682 74. Biller, S. J., Berube, P. M., Lindell, D. & Chisholm, S. W. Prochlorococcus: the structure and
683 function of collective diversity. *Nat. Rev. Microbiol.* **13**, 13–27 (2015).
684 75. Chaumeil, P.-A., Mussig, A. J., Hugenholtz, P. & Parks, D. H. GTDB-Tk: a toolkit to classify
685 genomes with the Genome Taxonomy Database. *Bioinformatics* (2019)
686 doi:10.1093/bioinformatics/btz848.
687 76. Pachiadaki, M. G. *et al.* Charting the Complexity of the Marine Microbiome through Single-

688 Cell Genomics. *Cell* **179**, 1623–1635.e11 (2019).
689 77. Nordberg, H. *et al.* The genome portal of the Department of Energy Joint Genome Institute:
690 2014 updates. *Nucleic Acids Res.* **42**, D26–31 (2014).
691 78. Eddy, S. R. Accelerated Profile HMM Searches. *PLoS Comput. Biol.* **7**, e1002195 (2011).
692 79. Sievers, F. & Higgins, D. G. Clustal Omega for making accurate alignments of many protein
693 sequences. *Protein Sci.* **27**, 135–145 (2018).
694 80. Capella-Gutiérrez, S., Silla-Martínez, J. M. & Gabaldón, T. trimAl: a tool for automated
695 alignment trimming in large-scale phylogenetic analyses. *Bioinformatics* **25**, 1972–1973
696 (2009).
697 81. Nguyen, L.-T., Schmidt, H. A., von Haeseler, A. & Minh, B. Q. IQ-TREE: a fast and effective
698 stochastic algorithm for estimating maximum-likelihood phylogenies. *Mol. Biol. Evol.* **32**,
699 268–274 (2015).
700 82. Minh, B. Q., Nguyen, M. A. T. & von Haeseler, A. Ultrafast approximation for phylogenetic
701 bootstrap. *Mol. Biol. Evol.* **30**, 1188–1195 (2013).
702 83. Kalyaanamoorthy, S., Minh, B. Q., Wong, T. K. F., von Haeseler, A. & Jermiin, L. S.
703 ModelFinder: fast model selection for accurate phylogenetic estimates. *Nat. Methods* **14**,
704 587–589 (2017).
705 84. Letunic, I. & Bork, P. Interactive Tree Of Life (iTOL) v4: recent updates and new
706 developments. *Nucleic Acids Res.* **47**, W256–W259 (2019).
707 85. Salichos, L., Stamatakis, A. & Rokas, A. Novel information theory-based measures for
708 quantifying incongruence among phylogenetic trees. *Mol. Biol. Evol.* **31**, 1261–1271 (2014).
709 86. Lartillot, N., Lepage, T. & Blanquart, S. PhyloBayes 3: a Bayesian software package for
710 phylogenetic reconstruction and molecular dating. *Bioinformatics* **25**, 2286–2288 (2009).
711 87. Thorne, J. L., Kishino, H. & Painter, I. S. Estimating the rate of evolution of the rate of
712 molecular evolution. *Mol. Biol. Evol.* **15**, 1647–1657 (1998).
713 88. Smith, S. A. & O'Meara, B. C. treePL: divergence time estimation using penalized likelihood
714 for large phylogenies. *Bioinformatics* **28**, 2689–2690 (2012).
715 89. Stamatakis, A. RAxML version 8: a tool for phylogenetic analysis and post-analysis of large
716 phylogenies. *Bioinformatics* **30**, 1312–1313 (2014).
717 90. Lechner, M. *et al.* Proteinortho: detection of (co-)orthologs in large-scale analysis. *BMC*
718 *Bioinformatics* **12**, 124 (2011).

91. Kanehisa, M. & Goto, S. KEGG: kyoto encyclopedia of genes and genomes. *Nucleic Acids Res.* **28**, 27–30 (2000).
92. Kanehisa, M. Toward understanding the origin and evolution of cellular organisms. *Protein Sci.* **28**, 1947–1951 (2019).
93. Kanehisa, M., Furumichi, M., Sato, Y., Ishiguro-Watanabe, M. & Tanabe, M. KEGG: integrating viruses and cellular organisms. *Nucleic Acids Res.* **49**, D545–D551 (2021).
94. Revell, L. J. phytools: an R package for phylogenetic comparative biology (and other things). *Methods in Ecology and Evolution* vol. 3 217–223 Preprint at https://doi.org/10.1111/j.2041-210x.2011.00169.x (2012).
95. Bollback, J. P. SIMMAP: stochastic character mapping of discrete traits on phylogenies. *BMC Bioinformatics* **7**, 88 (2006).
96. Brasier, M. D. & Lindsay, J. F. A billion years of environmental stability and the emergence of eukaryotes: new data from northern Australia. *Geology* **26**, 555–558 (1998).
97. Butterfield, N. J. *Bangiomorpha pubescens*n. gen., n. sp.: implications for the evolution of sex, multicellularity, and the Mesoproterozoic/Neoproterozoic radiation of eukaryotes. *Paleobiology* vol. 26 386–404 Preprint at https://doi.org/10.1666/0094-8373(2000)026<0386:bpngns>2.0.co;2 (2000).
98. Moczydłowska, M. Paleobiology of the neoproterozoic svanbergfjellet formation, spitsbergen. *Palaeogeography, Palaeoclimatology, Palaeoecology* vol. 122 247–248 Preprint at https://doi.org/10.1016/0031-0182(96)85042-5 (1996).